

Technical Paper

Investigation on quality of thin concrete cover using mercury intrusion porosimetry and non-destructive tests

Liyanto EDDY*, Koji MATSUMOTO, Kohei NAGAI, Piyaphat CHAEMCHUEN,
Michael HENRY and Kota HORIUCHI

(Received: January 17, 2018; Accepted: May 10, 2018; Published online: July 03, 2018)

Abstract: Mercury intrusion porosimetry test was carried out to investigate the quality of thin concrete cover. Specimens with different water-to-cement ratios were prepared and exposed to different environmental conditions. The results show that the pore structure of the cover is coarser than that of the center portion when the cover is insufficient. With thinner cover, the pore structure becomes coarser. With decreasing water-to-cement ratio, the pore structure becomes finer, and the difference in the pore structure between the cover and the center portion becomes smaller. If the cover is insufficient, not only the distance needed for substances to reach the bar becomes shorter, but also the pore structure becomes coarser. At 91 days, the pore structures of outdoor specimens are almost the same as those of indoor specimens although the exposure conditions are different. To investigate the applicability of the air permeability test and electric resistivity test to evaluate the cover quality when the cover is insufficient, specimens with different water-to-cement ratios and cover depths were prepared. A combination of the air permeability test and electric resistivity test roughly pointed out the poor quality of the insufficient concrete cover and is a useful technique to evaluate the concrete cover in real structures.

Keywords: cover, quality, permeability, porosity, resistivity, durability.

1. Introduction

The durability of infrastructures has become a major concern in some countries because insufficient concrete cover was found due to the poor quality of the construction. Among six structures along the North Sea coast in The Netherlands investigated by Polder and De Rooij [1], only one structure had corrosion damage related to the relatively low cover depths. Moradi-Marani et al. [2] reported that the jetty structure located in the northern coast of Persian Gulf, north of Strait of Hormoz, near the port of Bandar-Abbas underwent major corrosion rehabilitation after 7 years of service because the

inadequate cover thickness for reinforced concrete elements intensified the corrosion rate. It is well understood that the insufficient concrete cover can lead to earlier corrosion initiation and easier spalling of concrete because the distance needed for the substances to reach the steel bar becomes shorter. On the other hand, if the concrete cover is too thin, the concrete properties over the reinforcing bars might be different because large aggregates cannot pass through this limited clearance and this layer is exposed directly to the environment as illustrated in Fig. 1.

To evaluate the quality of the concrete cover in the real structures, many non-destructive methods [3-5] have been proposed. Recently, the surface air permeability test proposed by Torrent [6-7] and the electric resistivity test [8-9] have become increasingly popular in used to evaluate the quality of the concrete cover. Previous experimental works [10-12] have shown that the surface air permeability coefficient can be correlated with the water absorption rate, carbonation depth, and the diffusion coefficient of the chloride ions. Meanwhile, the moisture content of the concrete and composition of the material influence the electric resistivity of the concrete [13,14]. The corrosion rate can also be con-

Corresponding author Liyanto EDDY is JSPS postdoctoral fellow of Institute of Industrial Science, The University of Tokyo, Japan.

Koji MATSUMOTO is a project assistant professor of Institute of Industrial Science, The University of Tokyo, Japan.

Kohei NAGAI is an associate professor of Institute of Industrial Science, The University of Tokyo, Japan.

Piyaphat CHAEMCHUEN is an undergraduate student of Chulalongkorn University, Thailand.

Michael HENRY is an associate professor of Hokkaido University, Japan.

Kota HORIUCHI an undergraduate student of Hokkaido University, Japan.

nected with the electric resistivity of the concrete [15]. However, if the local differences in the concrete properties over the reinforcing bar exist in the case of the thin cover depth, the applicability of the non-destructive tests to the presence of this local zone should be clarified.

There are two ultimate purposes in this study. The first is to investigate the effect of the thin concrete cover on the concrete durability. Porosity and pore structure play an important role in the durability of concrete, and Mercury intrusion porosimetry (MIP) has been widely used for porous space investigation. In this study, MIP test was conducted to evaluate the pore structure of the concrete over the reinforcing bar in the case of the insufficient concrete cover. The change of the pore size distribution over time and the variation of the pore size distribution due to different exposure conditions (i.e., indoors and outdoors) are also discussed in this study. In the reality, real reinforced concrete structures are always exposed to the natural environment. However, the temperature and humidity outdoors are far more complex than those in the experimental room. Therefore, the indoor condition was selected because the temperature is relatively easy to control. Meanwhile, the second is to investigate the applicability of the non-destructive tests to evaluate the concrete cover quality of the real structures in the future considering the insufficient concrete cover. In this series, the specimens were also exposed to different conditions (i.e., indoors and outdoors).

2. Experimental program of MIP measurement

2.1 Materials

Concrete was prepared using tap water (W), type-I Portland cement (C), river sand (S), coarse aggregates (G), and air-entraining (AE) admixtures. Concrete mix proportions and fresh concrete properties are given in Table 1. Two different water-to-cement ratios which were 0.45 and 0.6 were selected for this experimental investigation. The maximum size of the coarse aggregate was 20 mm.

2.2 Preparation of specimens

To investigate the effect of the thin concrete cover because of the poor construction quality on

the concrete cover properties, four reinforced concrete specimens were prepared. The specimens were 200 mm×100 mm×200 mm in size reinforced with three deformed steel bars of 19.1 mm diameter (D19) at cover depths of 5, 15, and 30 mm as shown in Fig. 2. Cover depth of 5 mm was selected to represent the extremely poor quality of the construction, while cover depth of 15 mm illustrated the poor quality of the construction. Meanwhile, cover depth of 30 mm represented the fairly poor quality of the construction. It was assumed that when the concrete cover is sufficient which is more than 40 mm, the concrete properties of the concrete cover might be the same as the those of the center portion. To form a flat top surface, the specimens were cast with the specimens orientated upside down illustrated in Fig. 2(b). The formwork was filled in two equal layers, and every layer was compacted for 5 seconds with a handheld concrete vibrator.

The specimens were demoulded one day after casting, wrapped in the wet clothes and cured for seven days. At the end of the curing, the wet clothes were removed, and the specimens were exposed to different exposure conditions. Only top surface of the specimens was exposed, while other surfaces of the specimens were sealed with plastic wrap. Two specimens with different water-to-cement ratios were kept in the laboratory at a temperature of 20 °C. Meanwhile, other two specimens with different water-to-cement ratios were stored in outdoors and exposed to natural sunlight in Tokyo, Japan. Furthermore, the temperature and humidity were also recorded every hour using a temperature and humidity data logger as shown in Fig. 3.

2.3 Experimental method using MIP

MIP is one of the most widely used methods to study the pore structure of cementitious materials based on the physical principle that a non-reactive, non-wetting liquid will only penetrate fine pores when a sufficient pressure is applied to allow it to intrude. An increasing pressure is required to force mercury into pores of decreasing size. The imposed pressure is converted to the equivalent pore diameter using the Washburn equation [9] as in Eq. (1).

Table 1 – Concrete mix proportions and properties

W/C	Water (kg/m ³)	Cement (kg/m ³)	Sand (kg/m ³)	Gravel (kg/m ³)	AE (kg/m ³)	Slump (cm)	Air content (%)	91-day comp. strength (MPa)
0.45	168.6	378	735	1032	1.42	8.8	4.1	49.51
0.60	168.9	283	823	1023	1.1	8.3	3.0	38.60

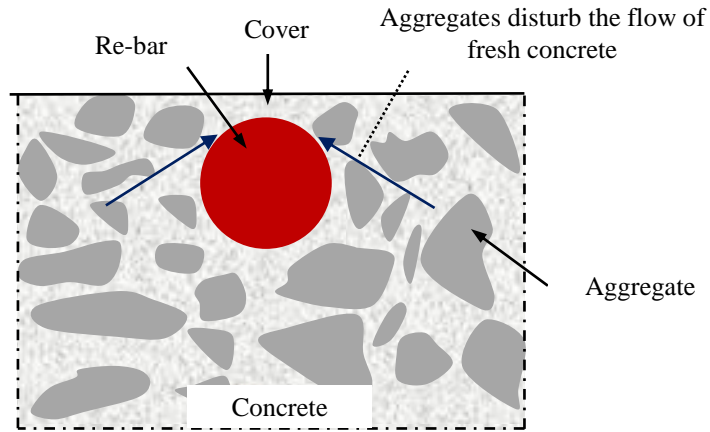
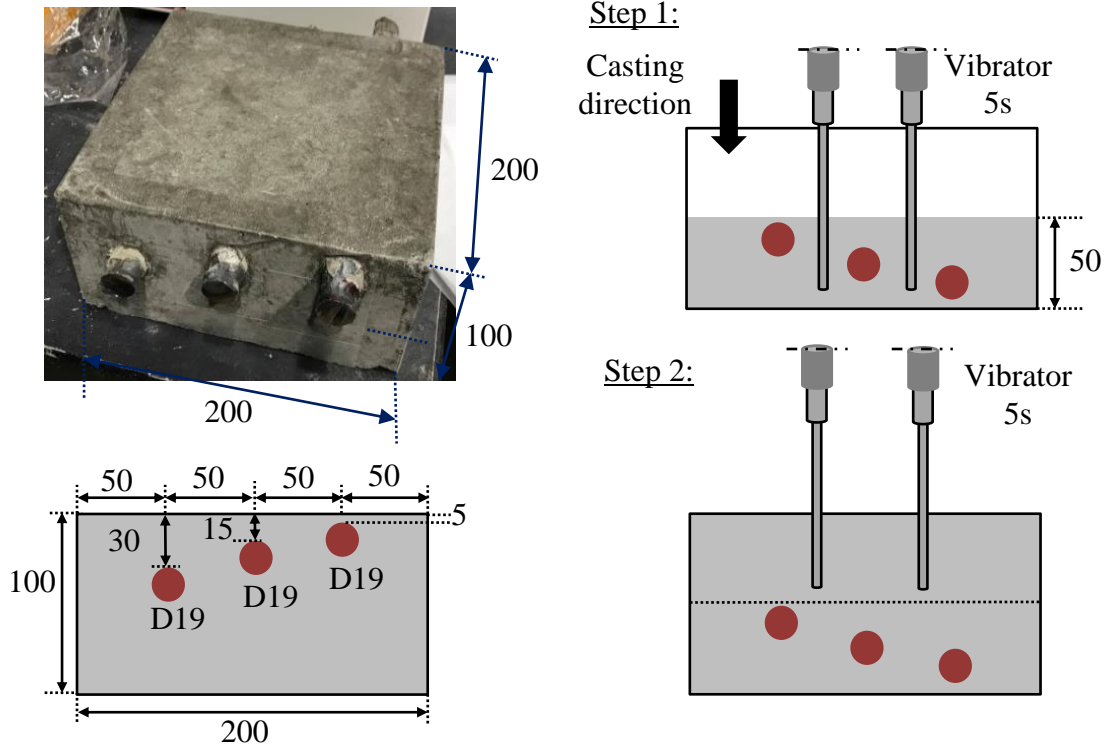


Fig. 1 – Illustration of insufficient concrete cover



(a) Detail of the specimens

(b) Casting procedure

Fig. 2 – Outline of experimental specimens for MIP test (units: mm)



Fig. 3 – Temperature and humidity data logger

$$D = -(4\gamma\cos\theta/P) \quad (1)$$

where D is the diameter of the pore (m), P is the applied pressure (Pa), θ is the contact angle between liquid mercury and the pore wall which is assumed to be 130° , γ is the surface tension of the mercury which is assumed to be 0.48 N/m .

Previous experiments [16-17] reported that there was a correlation between threshold pore size which is an indicator of pore structure and the diffusion coefficient of oxygen and chloride ions in cement pastes. Here, threshold pore size is the minimum pore size which mass should pass to penetrate the objective and pore size distribution is measured with MIP.

At 7, 14, 28, and 91 days after the casting, a 20-mm thick piece from one end of the specimens was cut with a water-cooled, diamond-bladed saw as illustrated in Fig. 4. Cubic pieces, approximately 5 millimeters in size, were taken from each piece at four different locations which are above each reinforcing bar and at the center portion of the piece, as shown in Fig. 5. The samples at the center of the piece served as the reference. The samples consist of only mortar pastes, and coarse aggregates were excluded in all samples. The samples were submerged in acetone for 24 hours to stop the hydration reaction, and then dried using a D-dry vacuum pump. After drying, a sample, approximately 1.5 grams in weight and consisting of the cubic pieces from the same location, was placed inside a sample cell for the MIP test. The maximum pressure applied was 130 MPa. For each testing age, in a total of 20 samples with different water-to-cement ratios, exposure conditions, and locations were tested.

3. Results of MIP test

3.1 Environmental conditions

As shown in Fig. 6(a) the measured hourly temperature inside the experimental room was almost constant. The specimens in the experimental room were exposed a temperature of 20°C and the relative humidity (RH) ranging from 45% to 93%. Meanwhile, the specimens stored in outdoors were exposed to fluctuating temperature and relative humidity. After 7 days of curing, two specimens with different water-to-cement ratios were removed and the exposure to the natural environment was started in summer. The specimens stored in outdoors were exposed to relatively high temperature and low humidity in the summer from day 7 to day 14 depicted in Fig. 6(b).



Fig. 4 – Specimen cut with a water-cooled, diamond-bladed saw

Samples at the surface of the concrete cover of 30 cm were taken only at 91 days in the case of 0.60 of water-to-cement ratio.

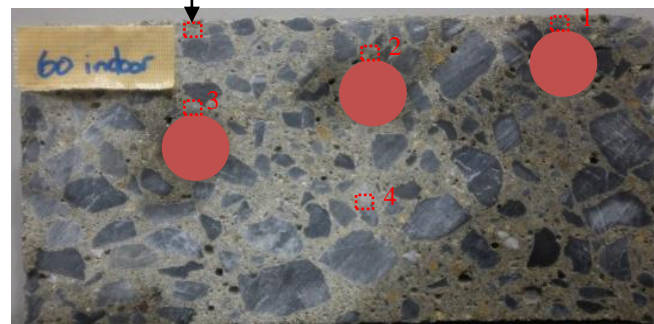


Fig. 5 – Sample locations for MIP test

The environment temperature ranged from 23.1°C (night) to 38.5°C (day), while the relative humidity ranged from 39.4% to 100%, and rain rarely fell during this period. From day 14 to day 28, the temperature ranged from 21.4°C (night) to 40.7°C (day) which is still relatively high, but rain fell several times during this period. The relative humidity ranged from 36.2% to 100%. Because of the season change from summer to fall, the temperature decreased from day 28 to day 91. The temperature ranged 17.3°C (night) to 39°C (day), while the humidity ranged from 33.4%-100%. Furthermore, the rain fell almost every day at the end of this period.

3.2 Porosity for W/C=0.60

Figures 7 and 8 present the cumulative pore-size distribution curves and the derivatives of the curves to facilitate the interpretation of the MIP data for the series of 0.6 of water-to-cement ratio at 7, 14, 28 and 91 days in the cases of specimens

stored in indoors and outdoors, respectively. Here, derivative $dV/d\log D$ is defined as a linear derivative of the cumulative pore volume curve with respect to the pore diameter. It is observed that the changes in pore structure over time vary depending on the exposure conditions. In the cases of the specimens stored in indoors, the cumulative pore-size distribution curves for the concrete over the reinforcing bar at cover depths of 5 mm and 15 mm show that the volume of the pores bigger than 500 nm in size decreases over time, while the main capillary pore peak is shifted to the bigger size especially for the concrete over the reinforcing bar cover depths of 5 mm. It might be attributed to the effect of the drying. Meanwhile, the cumulative pore-size distribution curve for the concrete over the reinforcing bar at cover depth of 30 mm does not change significantly over time with the tendency that the capillary pore peak is shifted to the smaller size and the volume decreases. Deeper zone shows lower total porosities in which the dominant pore size becomes smaller indicating the finer pore structure. It indicates that in the case of insufficient concrete cover, the thin layer is affected directly by the exposure from the environmental condition.

At 91 days, samples were also taken from the surface of the concrete cover of 30 mm. The cumulative pore-size distribution curve and the derivatives of the curve are shown in Fig. 9. The curves are compared with the curves for the concrete over the reinforcing bars at cover depths of 5 mm and 30 mm. The total pore volume of the surface of the concrete cover of 30 mm is lower than that of the concrete over of 5 mm. The volume of the pores more than 150 nm in size of this zone is lower than that of the concrete cover of 5 mm, but the volume of the pores less than 150 nm in size of this zone is higher than that of the concrete cover of 5 mm. It indicates that the pore structure of the concrete cover of 5 mm is coarser than that of the surface of the concrete cover of 30 mm. It might be affected by the behavior of the concrete passing through the narrow spaces. When the concrete passes through the limited clearance, the blockage sometimes occurs resulting in the coarser pore structure. On the other hand, the cumulative pore-size distribution curve for the concrete at the center portion shifts to the left with increasing age especially from 28 days to 91 days. With increasing age, the dominant pore size becomes smaller. In addition, the dominant pore size for the concrete at the center portion is smaller than that for the concrete at the concrete cover indicating finer pore structure.

Meanwhile, in the case of the specimens stored in outdoors, from 7 days (after curing) to 14 days (after 7 days exposed to the natural environment), higher amount of total pore volume is observed particularly in the concrete over the reinforcing bar at cover depth of 5 mm. The main pore peak is broader and shifted to the bigger size (Fig. 8(a)) and large pores appear approximately between 200 nm and 2000 nm in size. In the concrete over the reinforcing bar at cover depth of 15 mm, large pores appear approximately between 100 nm and 1,000 nm in size, but the volume of the main pore decreases. The large pores in the concrete over the reinforcing bar at cover depth of 30 mm and at the center portion do not occur as much as those in the concrete over the reinforcing bars at cover depths of 5 mm and 15 mm. This phenomenon might be attributed to drying since from 7 days to 14 days, and the effect is more significant than in the case of the specimens stored in indoors because the specimens stored in outdoors were exposed to relatively high temperature in summer. Furthermore, it indicates that the concrete exposed directly to the environment which is concrete at the top layer is affected significantly. After 14 days, increased time results in lower total porosities. The volume of main pores decreases, and the dominant pore size becomes smaller indicating hydration proceeds. Empty capillary pores because of the previous drying might be re-filled with water supply from rainfall. As a result, the porosity becomes finer because hydration proceeds. At 91 days, although the specimens were exposed to different exposure conditions, the cumulative pore-size distribution curves and the derivatives of the curves for the specimens stored in outdoors are almost the same as those for the specimens stored in indoors. The same tendency as the specimens stored in indoors is observed that the dominant pore size for the concrete at the center portion is smaller than that for the concrete at the concrete cover indicating finer pore structure.

It can be seen clearly that deeper zone shows finer pore structure for both specimens stored in outdoors and indoors. If the pore structure of the concrete cover is taken as the average over the depth of the concrete cover, the pore structure of concrete cover of 5 mm is the coarsest. The pore structure of concrete cover of 5 mm is coarser than that of concrete cover of 15 mm, and the pore structure of concrete cover of 15 mm is coarser than that of concrete cover of 30 mm. The pore structure at the center portion of the specimens is the finest. In addition, with thinner concrete cover, the dominant pore size becomes larger.

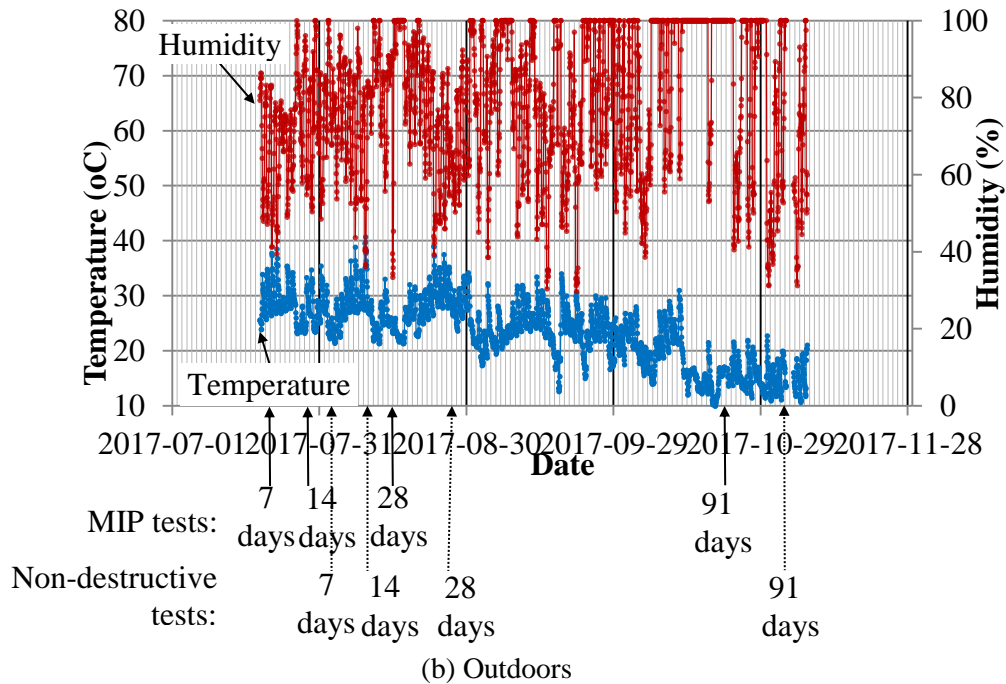
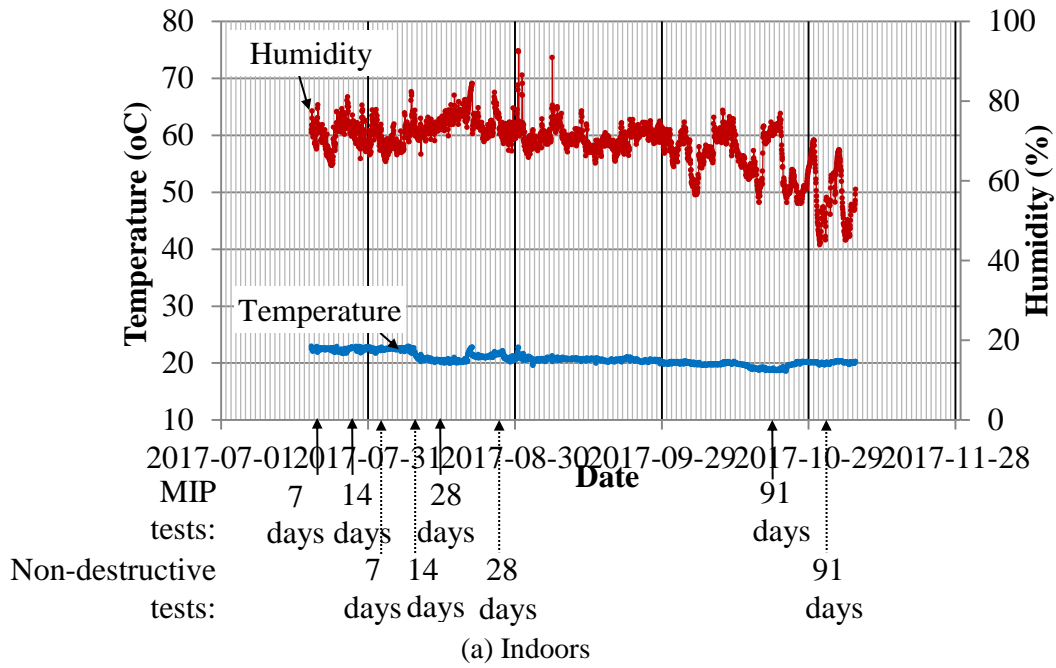


Fig. 6 – Measured hourly temperature and humidity

3.3 Porosity for W/C=0.45

A similar set of results is presented in Figs. 10 and 11 for the corresponding 0.45 of water-to-cement ratio. With lower water-to-cement ratio results in the lower total porosities. The same tendency is observed that although the changes in pore structure over time vary depending on the exposure conditions, the cumulative pore-size distribution curves and the derivatives of the curves for the specimens stored in outdoors are the same as those for the specimens stored in indoors at 91 days. The effect of the drying because of the high temperature

in summer in the case of 0.45 of water-to-cement ratio is not as significant as in the case of 0.60 of water-to-cement ratio. It can be seen clearly that, the insufficient concrete cover results in coarser pore structure. However, as the water-to-cement ratio was lower, the pore structures of concrete over the reinforcing bars at cover depth of 5 mm, 15 mm, and 30 mm are almost the same, but they are coarser than the pore structure at the center portion of the specimens. The dominant pore size for the concrete becomes smaller as the concrete cover is thicker.

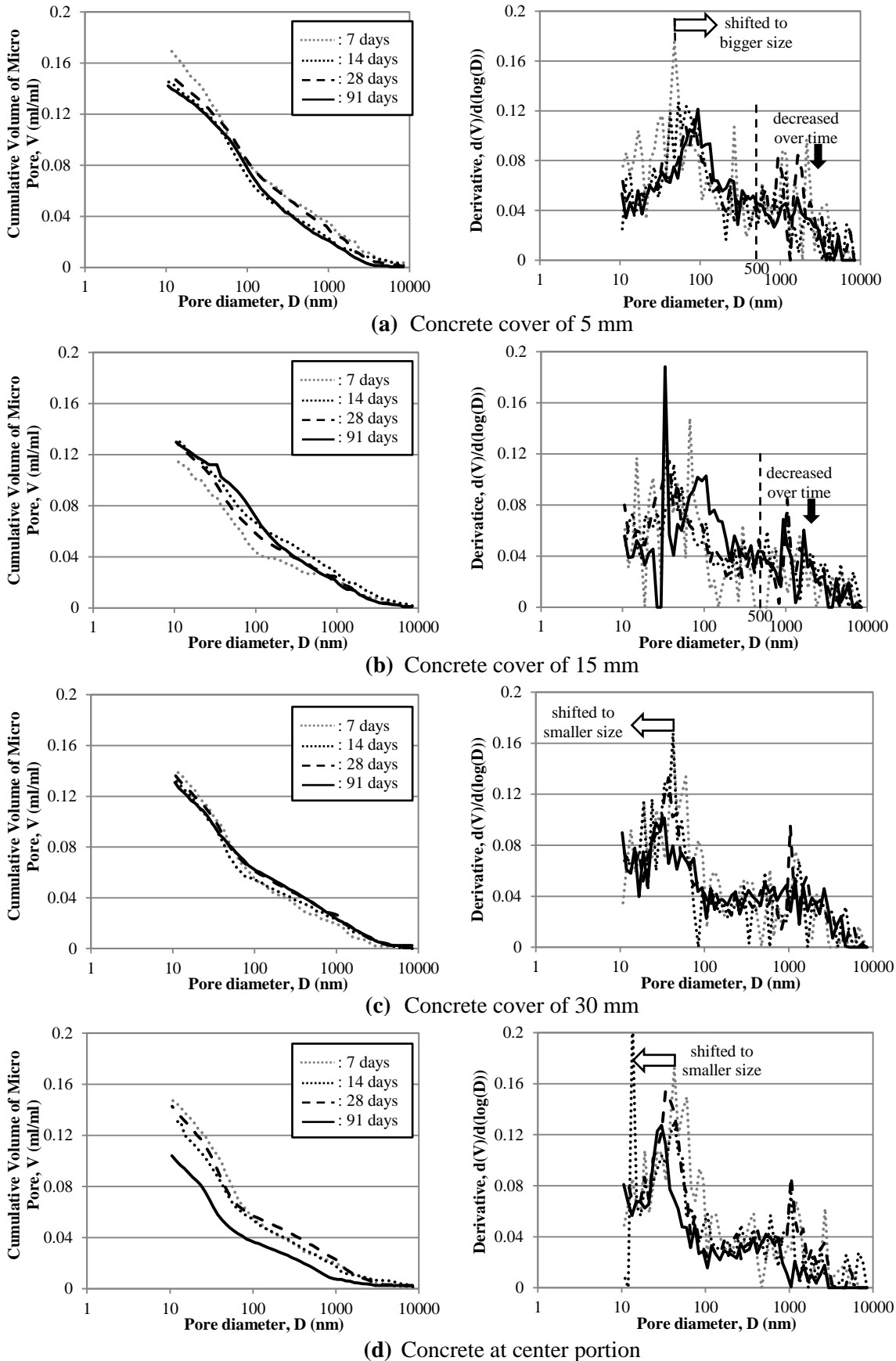


Fig. 7 – The cumulative pore-size distribution curves and the derivatives of the curves for the series of 0.6 of water-to-cement ratio in the case of specimens stored indoors

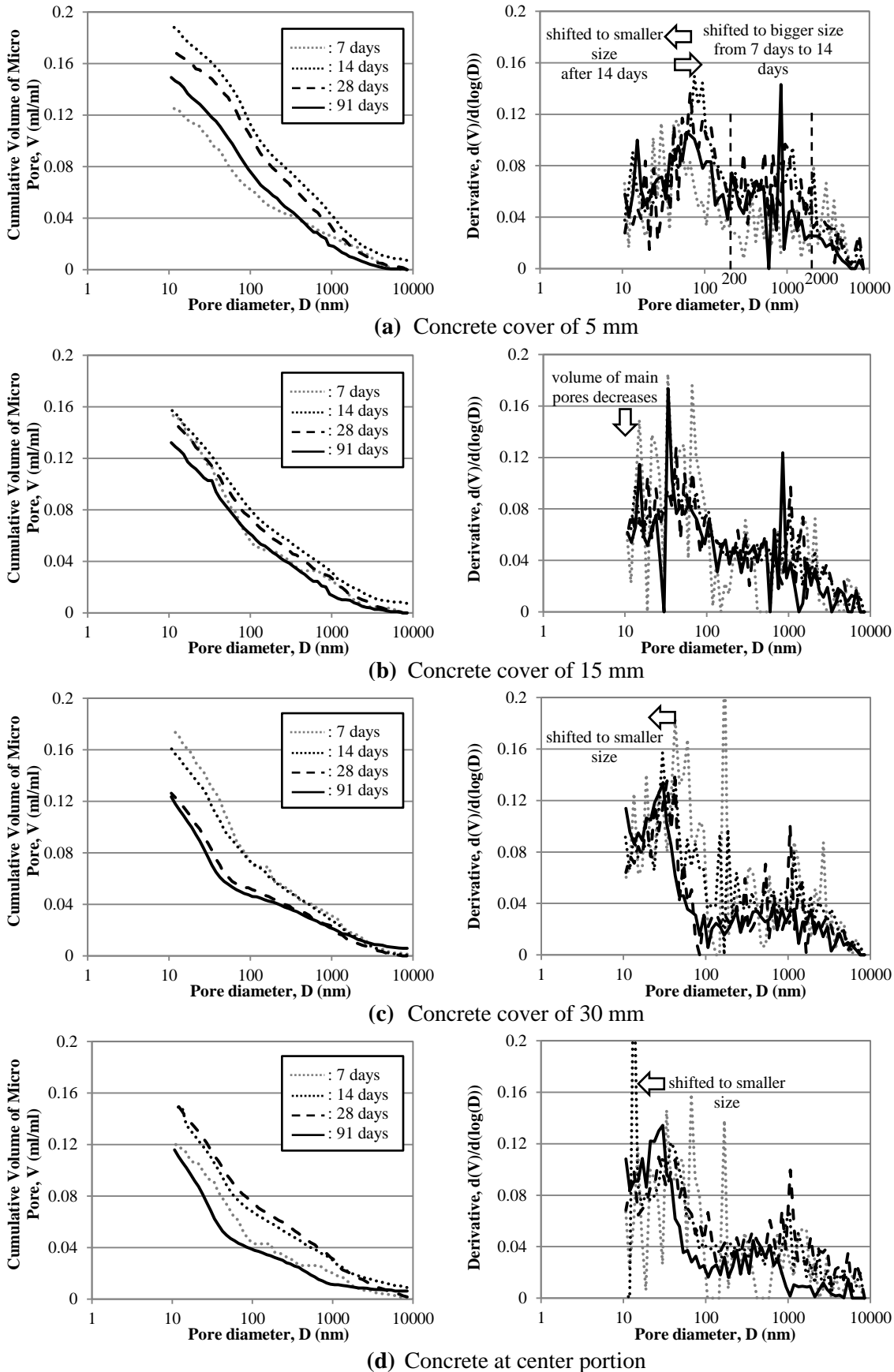
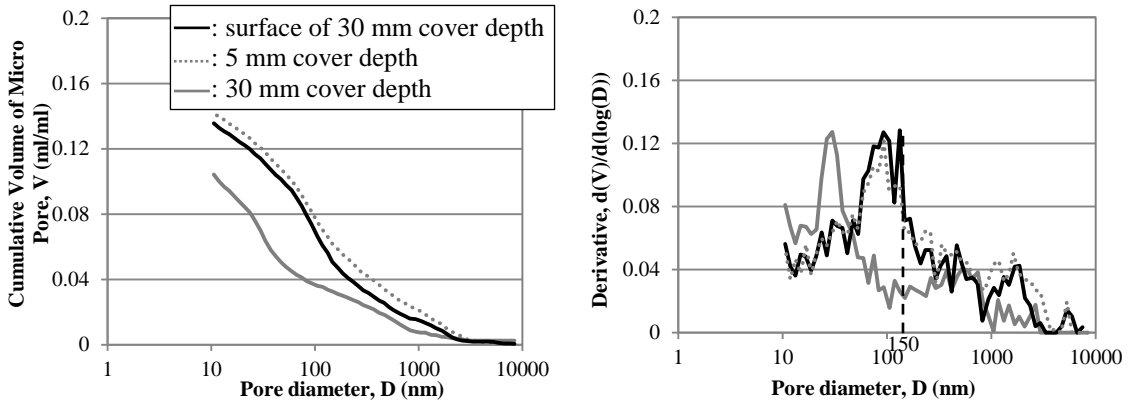
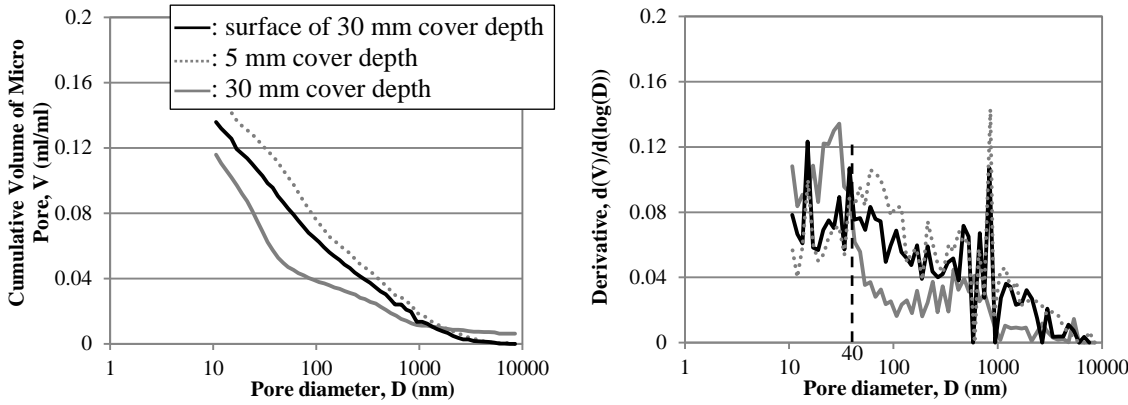


Fig. 8 – The cumulative pore-size distribution curves and the derivatives of the curves for the series of 0.6 of water-to-cement ratio in the case of specimens stored outdoors

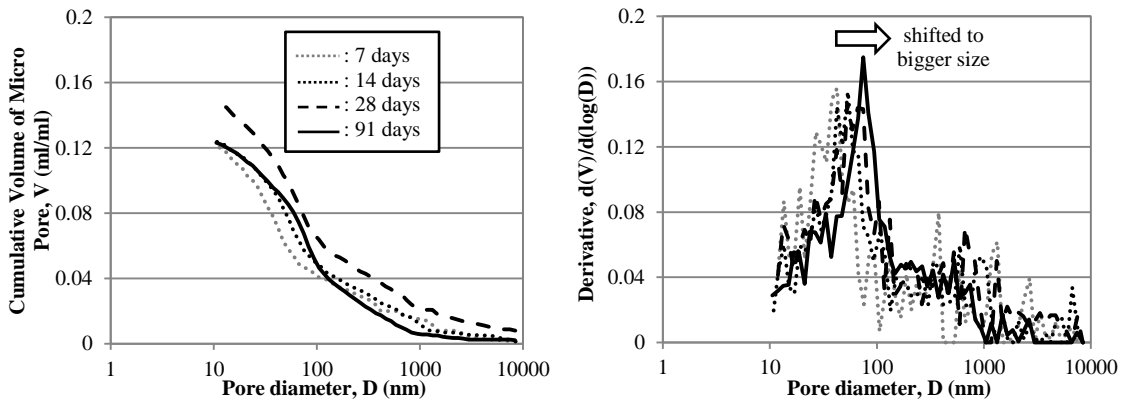


(a) Indoors

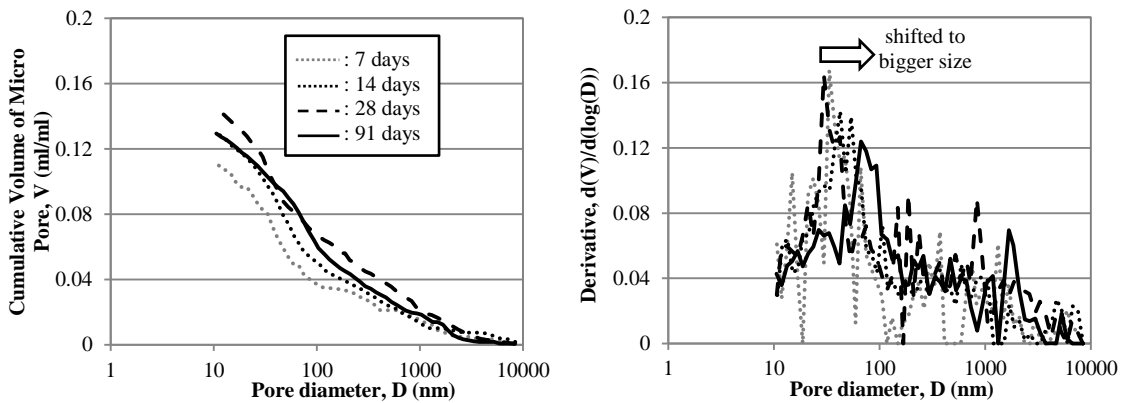


(b) Outdoors

Fig. 9 – The comparison of the cumulative pore-size distribution curves and the derivatives of the curves at 91 days between the surface of the concrete cover of 30 mm with the concrete over the reinforcing bars at depths of 5 mm and 30 mm.



(a) Concrete cover of 5 mm



(b) Concrete cover of 15 mm

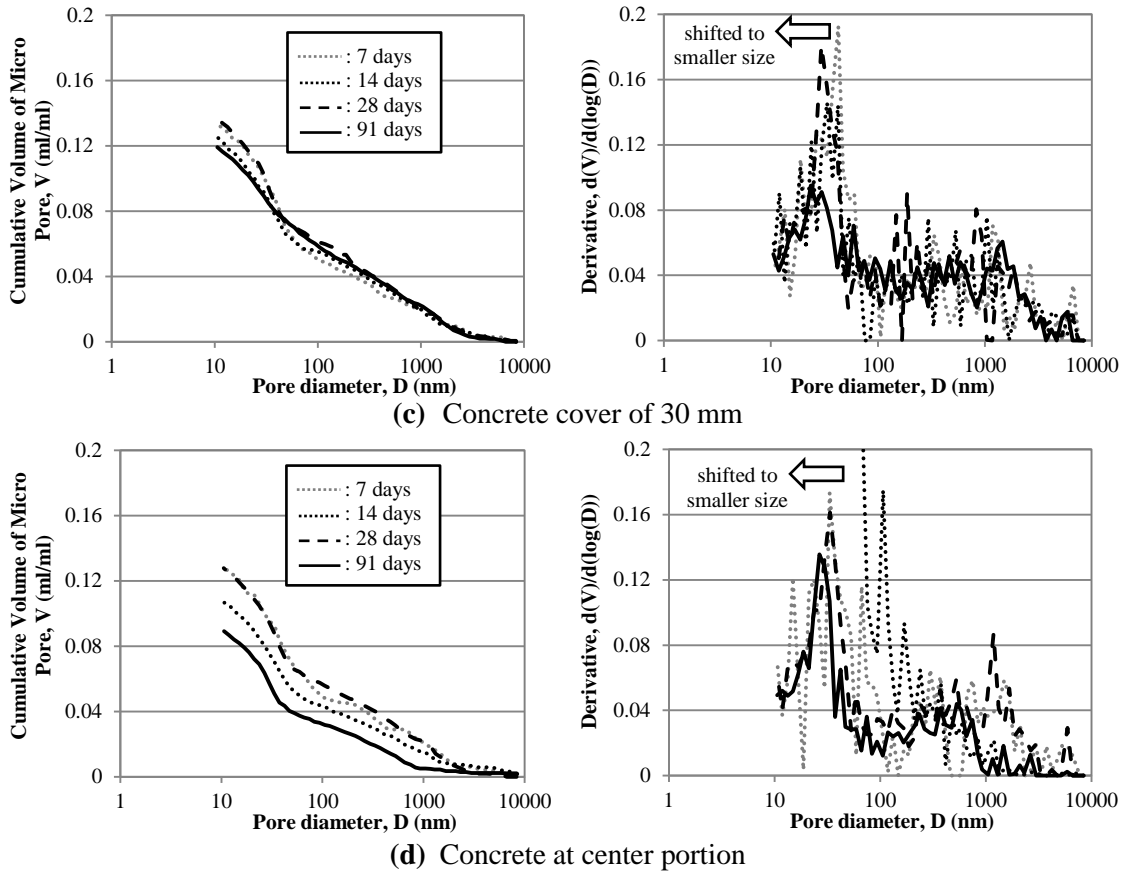


Fig. 10 – The cumulative pore-size distribution curves and the derivatives of the curves for the series of 0.45 of water-to-cement ratio in the case of specimens stored indoors

3.4 Durability aspect for insufficient concrete cover

As observed above, the thin concrete cover cases have different properties compared to other zones. The properties of the concrete over the reinforcing bar at cover depth of 5 mm are unknown. By comparing the porosity of different water-to-cement ratio, the equivalent properties are identified. To illustrate the equivalent properties, the comparison of the pore structure is made between the concrete over the reinforcing bar at cover depth of 5 mm in the case of 0.45 of water-to-cement ratio and the concrete at the center portion in the case of 0.60 of water-to-cement ratio. As shown in Fig. 12, the properties of the thin concrete cover in the case of 0.45 of water-to-cement ratio should be considered as the concrete properties with the water-to-cement ratio which is higher than 0.60. Therefore, when the concrete cover is insufficient, not only the distance needed for the substances to reach the steel bar becomes shorter, but also the pore structure becomes coarser than in the case of sufficient concrete cover. It should be pointed out that the diffusion coefficient increases exponentially with the water-to-cement ratio. For comparison purpose, using JSCE equation [18] given in Eq. (2), the diffusion

coefficient for 0.45 of water-to-cement ratio is 0.892 cm²/yr, while the diffusion coefficient for 0.60 of water-to-cement ratio is 2.606 cm²/yr. As a result, the service life of the real structures becomes shorten significantly.

$$\log D_c = -3.9(w/c)^2 + 7.2(w/c) - 2.5 \quad (2)$$

where D_c : diffusion coefficient of concrete (cm²/yr), w/c: water-to-cement ratio.

4. Experimental program of non-destructive tests

4.1 Materials

Concrete mix proportions and fresh concrete properties prepared for the non-destructive tests were the same as those used for the MIP test given in Table 1.

4.2 Preparation of specimens

To investigate the applicability of the air permeability test and electric resistivity test to evaluate the concrete cover quality when the concrete cover is insufficient, 22 cubic specimens, which were eight plain concrete specimens with different water-to-cement ratios and 14 reinforced concrete speci-

mens with different water-to-cement ratios and cover depths, were prepared. The experimental specimens are listed in Table 2. The specimens were 200 mm × 200 mm × 200 mm in size as illustrated in Fig. 13. As mentioned above, two water-to-cement ratios were used which were 0.45 and 0.60 for both plain and reinforced concrete specimens. In the case of the reinforced concrete specimens, a deformed steel bar of 19.1 mm diameter was embedded in each specimen with different cover depths which were 5, 15 and 30 mm. Cover depth of 5 mm was selected to represent the extremely poor quality of the construction and cover depth of 15 mm illustrated the poor quality of the construction. Meanwhile, cover depth of 30 mm represented the fairly poor quality of the construction. It was assumed that when the concrete cover is sufficient which is more than 40 mm, the concrete properties of the concrete cover might be the same as the those of the center portion. To form a flat top surface, the specimens were cast with the specimens orientated upside down illustrated in Fig. 13(b). The formwork was filled in two equal layers, and every layer was compacted for 5 seconds with a handheld concrete vibrator.

The specimens were demoulded one day after casting, wrapped in the wet clothes and cured for seven days. At the end of the curing, the wet clothes were removed, and the specimens were exposed to different exposure conditions. Four plain concrete specimens with different water-to-cement ratios and seven reinforced concrete specimens with different water-to-cement ratios and cover depths were kept in the laboratory at a temperature of 20°C, while the other four plain concrete specimens with different water-to-cement ratios and seven reinforced concrete specimens with different water-to-cement ratios and cover depths were stored in outdoors and exposed to natural sunlight in Tokyo, Japan. Furthermore, the temperature and relative humidity were also recorded every hour using a temperature and humidity data logger as shown in Fig. 3.

4.3 Experimental method using air permeability test and electric resistivity test

In the Torrent's method, a double-chamber cup is attached to a concrete surface by vacuum, and air in the pores of the surface layers of concrete, initially at atmospheric pressure, flows into the inner chamber causing its pressure to gradually increase. Based on a measured pressure growth and an assumption on the relevant porosity of concrete tested, the surface air permeability coefficient is calculated using Eq. (3).

$$k_T = \left(\frac{V_c}{A}\right)^2 \frac{\mu}{2\varepsilon P_a} \left(\frac{\ln \frac{P_a + \Delta P_{ieff}(t_f)}{P_a - \Delta P_{ieff}(t_f)}}{\sqrt{t_f} - \sqrt{t_o}}\right)^2 \quad (3)$$

where k_T : coefficient of air permeability (m^2), V_c : volume of inner cell system (m^3), A : cross-sectional area of inner cell (m^2), μ : viscosity of air ($= 2.0 \times 10^{-5} \text{ N.s/m}^2$), ε : estimated porosity of the concrete cover ($= 0.15$), P_a : atmospheric pressure (N/m^2), ΔP_{ieff} : effective pressure raise in the inner cell at the end of the test (N/m^2), t_f : time (s) at the end of the test, t_o : time (s) at the beginning of the test. The air permeability test was done at 7, 14, 28 and 91 days.

The measurements of the electric resistivity using the 4-point Wenner probe and the surface moisture content were also conducted as shown in Fig. 14. To measure the resistivity, the probe with four equally spaced point electors was pressed onto the concrete surface. The two outer electrodes induce the current, while the two inner electrodes measure the potential drop. The current flows through a volume of concrete with a depth approximately equal to the electrode distance a . The resistance obtained via this method can be converted to resistivity using a cell constant based on theoretical considerations using Eq. (4).

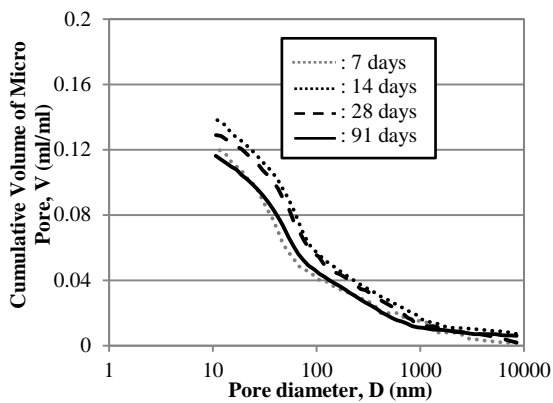
$$\rho = 2\pi a R \quad (4)$$

where a : the electrode spacing (cm), $R = \Delta V / I$ (Ω), ΔV : potential drop (V), I : current (A). In this study, the electric resistivity test was used to correct the air permeability coefficients [19-20].

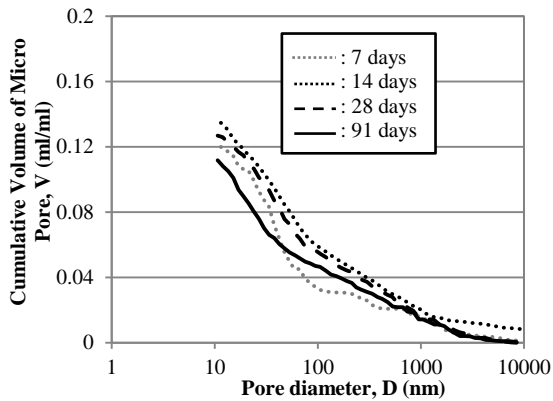
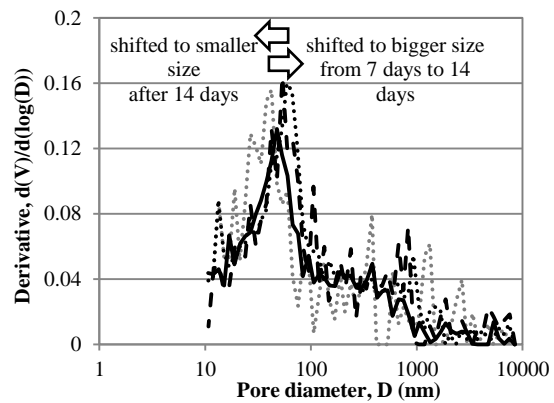
The importance of the moisture content of the concrete on the measured gas permeability is well known [21]. There is a possibility that the readings of the air permeability coefficients are affected by the in situ moisture content. To neutralize the effect of the moisture content, the combination of the air permeability test and electric resistivity test were proposed by Torrent et al. [19]. As pointed out by Kurashige et al. [20], the moisture content of concrete affects the measurement results of the Torrent's method. The air permeability test is just the volume of open pore in concrete which increases with moisture evaporation from concrete surface. To correct the effect of moisture content of concrete on the measurement results of the Torrent's method, the electric resistivity test was conducted. To measure the surface moisture content, the Tramex concrete encounter moisture meter was used. At the same time, the change in specimen mass was measured.

Table 2 – Number of experimental specimens in each case (non-destructive tests)

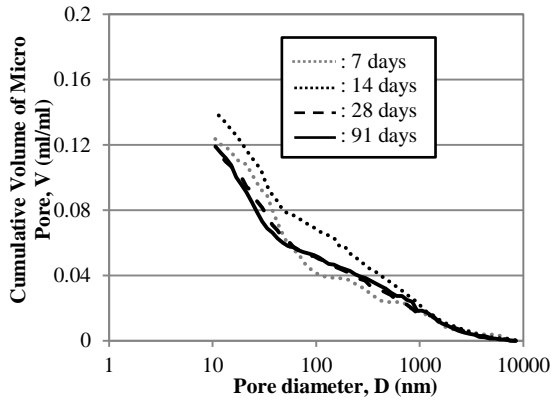
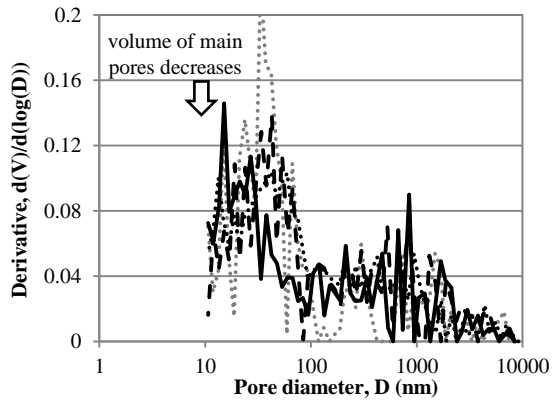
Exposure	W/C=0.45				W/C=0.60			
	Plain concrete	Reinforced concrete cover depth (mm)			Plain concrete	Reinforced concrete cover depth (mm)		
		5	15	30		5	15	30
Indoors	1	1	1	1	3	2	1	1
Outdoors	1	1	1	1	3	2	1	1



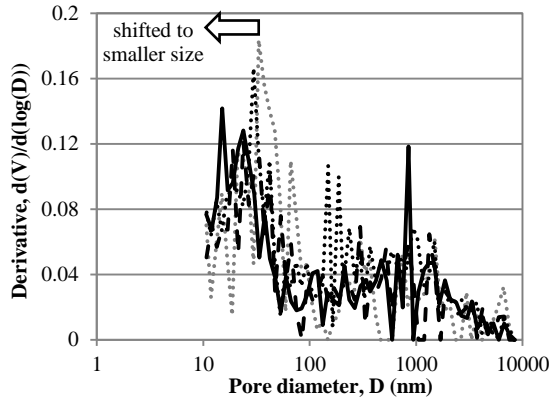
(a) Concrete cover of 5 mm

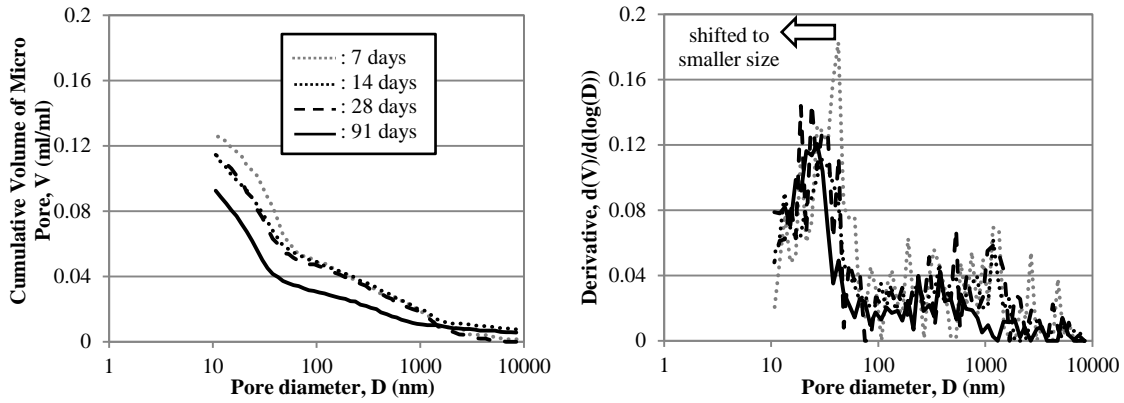


(b) Concrete cover of 15 mm



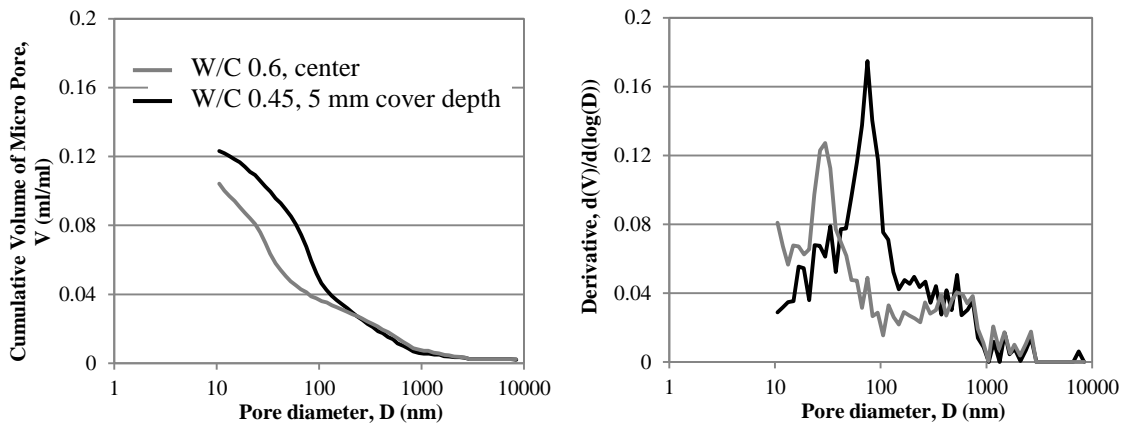
(c) Concrete cover of 30 mm



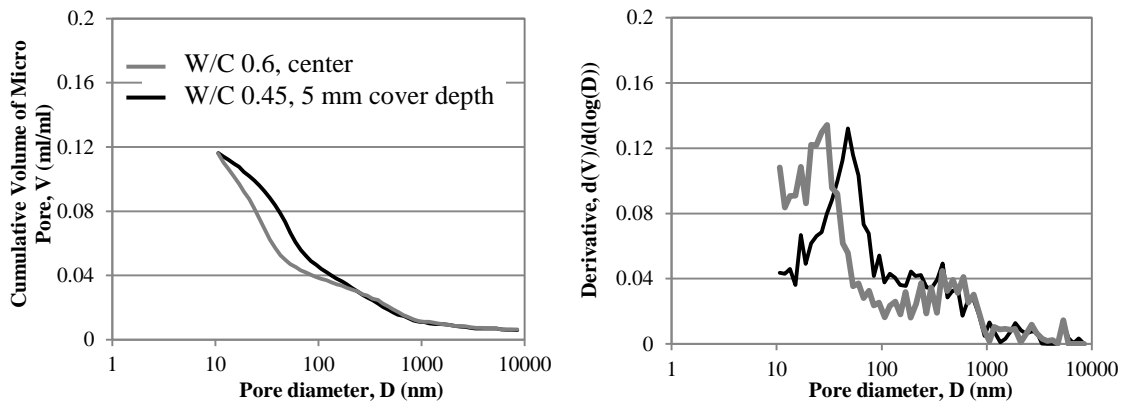


(d) Concrete at the center portion

Fig. 11 – The cumulative pore-size distribution curves and the derivatives of the curves for the series of 0.45 of water-to-cement ratio in the case of specimens stored outdoors



(a) Indoors



(b) Outdoors

Fig. 12 – The comparison of the cumulative pore-size distribution curves and the derivatives of the curves at 91 days between the concrete cover of 5 mm with 0.45 of water-to-cement ratio and concrete with 0.60 of water-to-cement ratio

5. Results of air permeability test and electric resistivity test

The specimens in this series are 10 days younger than those in the previous series. As shown in Fig. 6, the temperature and relative humidity in this series are almost the same as those in the previous series.

5.1 Mass loss

The mass of each specimen was measured at 7, 14, 28, and 91 days to have some reference data on the effect of rain and weather on the internal moisture content. The mass at 7 days was used as the original mass to quantify the mass loss or gain calculated using Eq. (5).

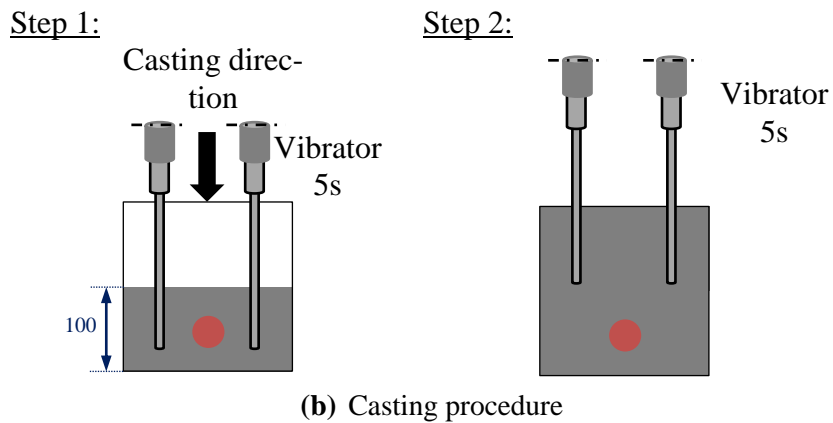
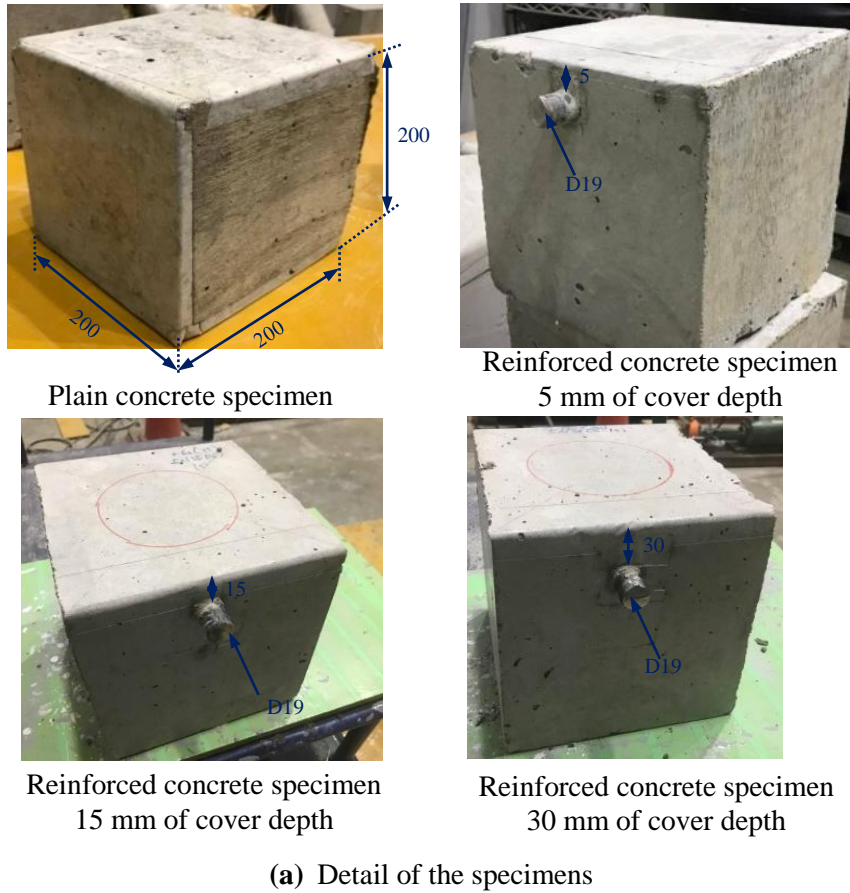


Fig. 13 – Outline of experimental specimens for non-destructive test (units: mm)

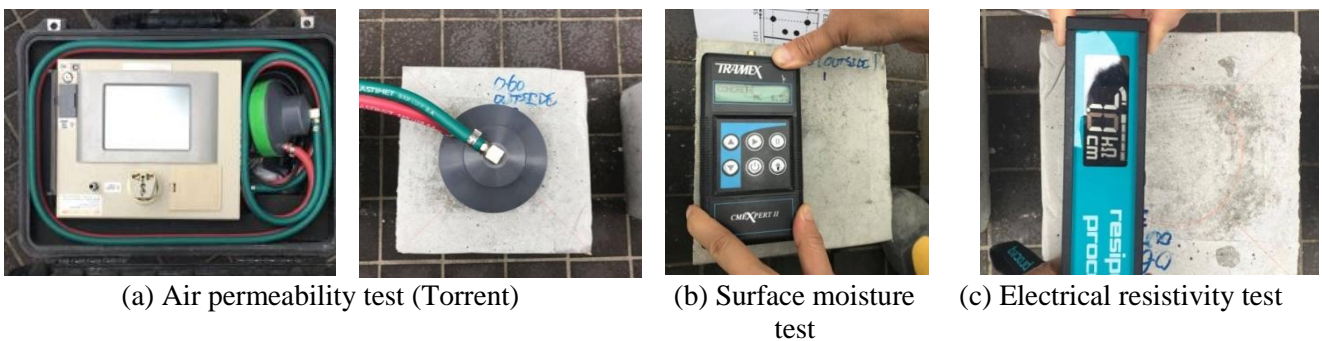


Fig. 14 – A set of non-destructive test proposed by Torrent et al. [19]

$$\Delta m = (m_7 - m_t) / m_7 \quad (5)$$

where Δm : mass loss ratio (%), m_7 : specimen mass at 7 days (kg), m_t : specimen mass at t days (kg).

Figure 15(a) depicts the change in mass for all specimens in the experimental room, while Fig. 15(b) depicts change in mass for all specimens kept outdoors. Positive value means that the specimen lost mass; while negative value means that the specimen gained mass. All specimens stored in the experimental room were always decreasing in mass indicating that all specimens indoors were exposed to drying conditions, and the moisture in the specimens was decreased over time. The moisture loss behavior in the early stage of drying was high because larger pores evaporate quicker than the smaller one. Meanwhile, all specimens stored in outdoors were decreasing in mass from 7 days to 14 days indicating drying conditions and the moisture in the specimens was decreased. However, they were increasing in mass after 14 days indicating the re-wetting from the rainfall water, and the moisture in the specimens was increased. All specimens show that with lower water-to-cement ratio, the change in mass becomes lower. This can be attributed to the fact that when water-to-cement ratio decreases, the pore network becomes finer.

5.2 Applicability non-destructive tests to evaluate the insufficient concrete cover

Figure 16(a) and (b) shows the change of the electric resistivities over time for all specimens stored in indoors and outdoors, respectively. As shown in Fig. 16(a), the electric resistivities for the specimens stored in indoors increase over time. The change in the electric resistivity over time for the specimens stored in indoors is in the same trend as the change in the mass over time. However, in the cases of the specimens stored in outdoors, the change in the electric resistivity over time is not in the same trend as the change in the mass over time. After 14 days, the masses increase over time indicating re-wetting from rainfall water, while the electric resistivities increase over time indicating the drying condition. It indicates that the moisture inside the concrete varies, and the electric resistivity test cannot penetrate to the deeper zone of the specimens.

Figure 17(a) and (b) shows the relationships between the air permeability test and the electric resistivity test results for all specimens stored in indoors and outdoors, respectively, at 91 days. As mentioned above, the electric resistivity test was also conducted to correct the air permeability meas-

urement as proposed by Torrent et al. [19]. Furthermore, Torrent et al. [19] proposed the classification of the concrete cover in Figs. 17(a) and (b). The experimental results show that the air permeability coefficients are in overall a good correlation with the water-to-cement ratios. With lower water-to-cement ratios, the air permeability coefficients become lower indicating better quality of the concrete cover. In the case of the specimens stored indoors, the quality of the specimens with water-to-cement ratio of 0.45 ranges from normal to bad, while the quality of the specimens with water-to-cement ratio of 0.60 ranges from normal to very bad. On the other hand, in the case of the specimens stored outdoors, the quality of the specimens with water-to-cement ratio of 0.45 ranges from very good to normal, while the quality of the specimens with water-to-cement ratio of 0.60 ranges from good to very bad.

The air permeability test roughly pointed out the existence of the poor quality of concrete cover in the cases of the insufficient concrete cover. The air permeability coefficients in the cases of 5 mm and 15 mm are higher than those in other cases. In the case of 0.60 of water-to-cement ratio, the quality of the concrete cover of 5 mm and 15 mm for the specimens stored indoors ranges from bad to very bad, while the quality of the concrete cover of 5 mm and 15 mm for the specimens stored outdoors ranges from normal to very bad. Meanwhile, in the case of 0.45 of water-to-cement ratio, the quality of the concrete cover of 5 mm and 15 mm for the specimens stored indoors ranges from normal to bad, while the quality of the concrete cover of 5 mm and 15 mm for the specimens stored outdoors ranges from very good to normal. However, the air permeability test results may overestimate the quality of the concrete cover because the concrete below the reinforcing bars where the concrete properties is better than the concrete over the reinforcing bars might be included in the measurement. Because the concrete below the reinforcing bar might be included in the measurement, the measured air permeability coefficient might be lower than if the test can measure only the air permeability coefficient of the concrete over the reinforcing bar.

Meanwhile, variations in the change of air permeability coefficients over time are observed due to different exposure conditions as shown in Fig. 18. The air permeability coefficients increase over time for the specimens stored in indoors. As discussed by Kurashige et al. [20], the change in the air permeability coefficients is affected by the moisture evaporation from the concrete surface because the moisture can block the air to flow into the chamber.

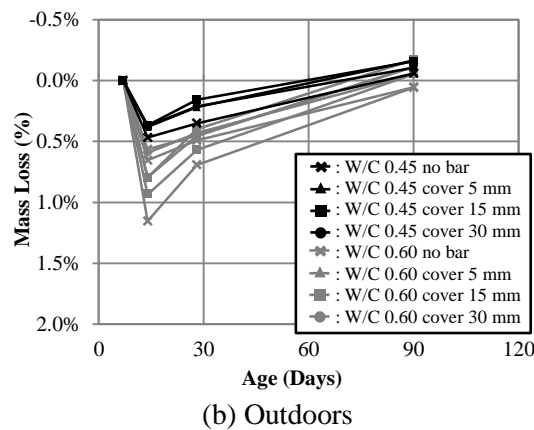
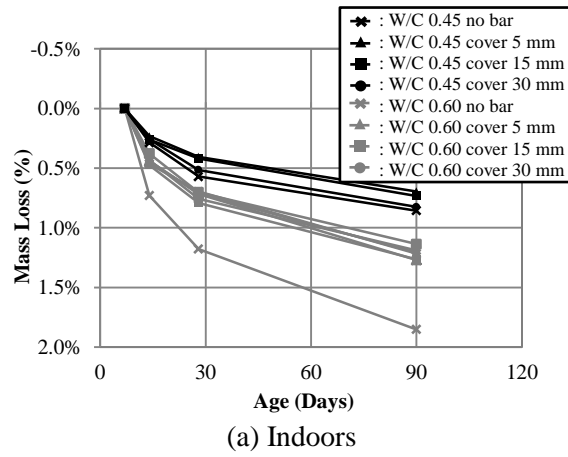


Fig. 15 – Mass loss over time

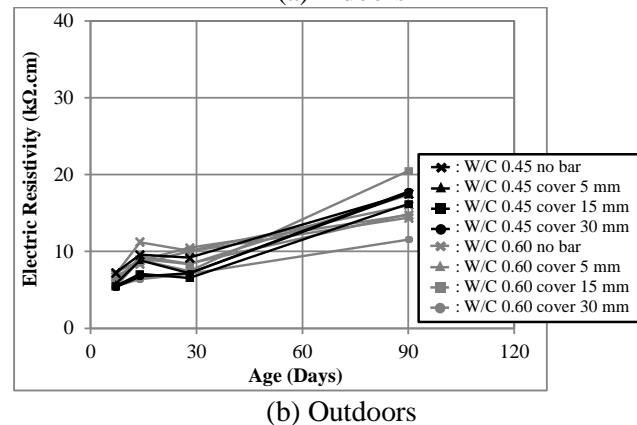
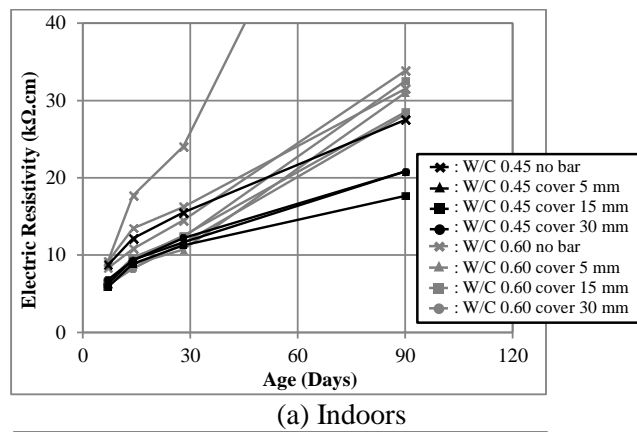


Fig. 16 – Electric resistivity over time

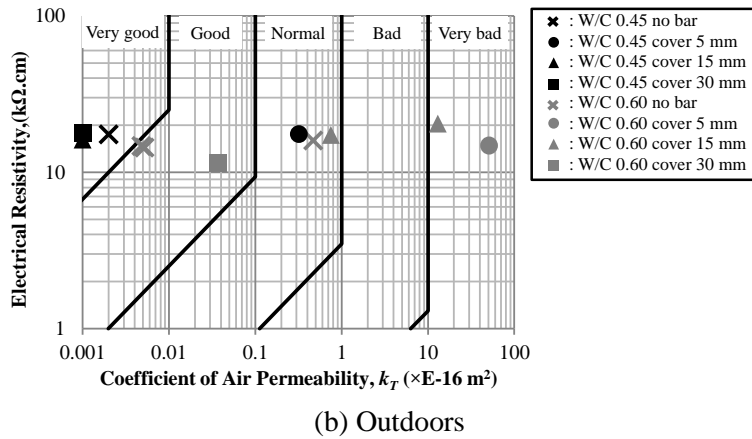
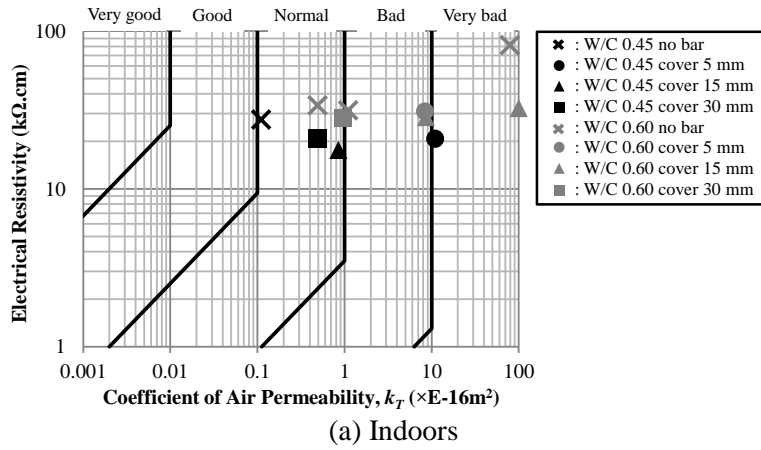


Fig. 17 – Relationships between air permeability coefficients and electric resistivity at 91 days for all specimens

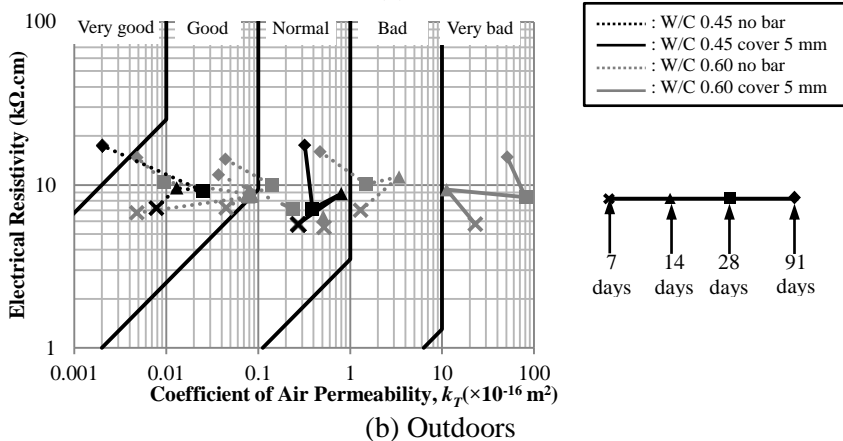
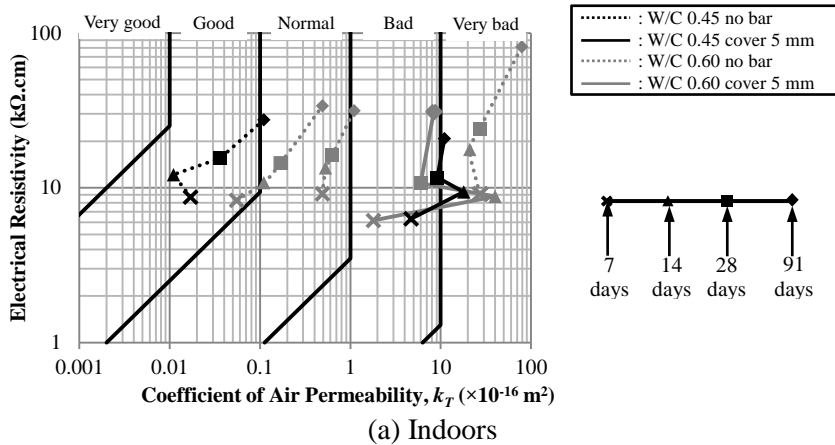


Fig. 18 – Relationships between air permeability coefficients and electric resistivity over time

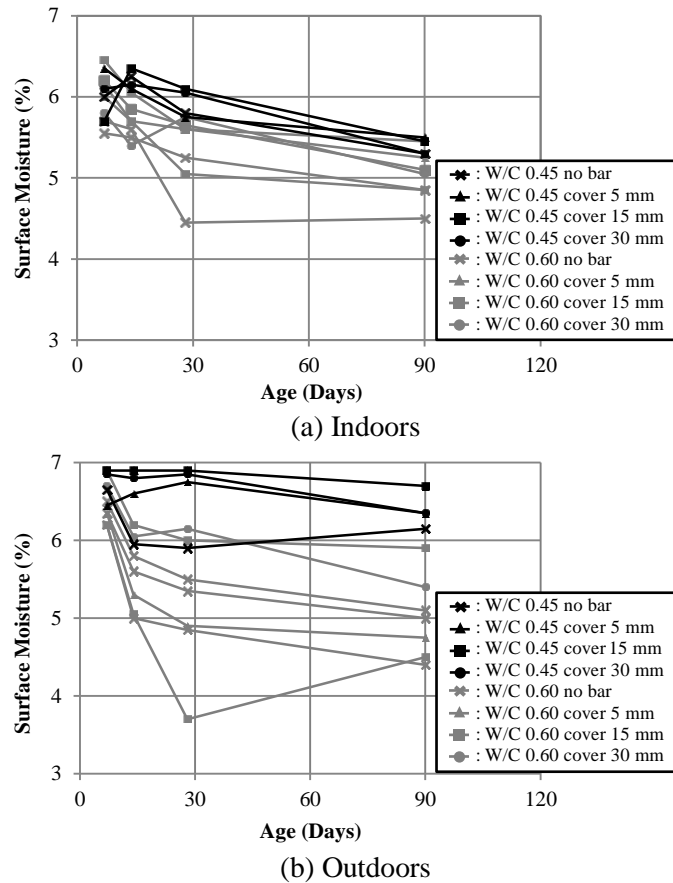


Fig. 19 – Surface moisture content over time

As depicted in Fig. 19 the surface moisture content decreases over time indicating the moisture evaporation from the concrete surface. However, in the cases of the specimens stored in outdoors, the air permeability coefficients increase from 7 days to 14 days, but after 14 days, the air permeability coefficients decrease over time. The change in air permeability coefficients over time is not in the same trend as the change in moisture content at the concrete surface in which the moisture at the concrete surface decreases over time as illustrated in Fig. 19. On the other hand, the change in the air permeability coefficients of the specimens stored in outdoors is in the same trend as the change in the mass over time. From 7 days to 14 days, as the masses decrease from 7 days to 14 days, the air permeability coefficients become higher. After 14 days, as the masses increase over time, the air permeability coefficients become lower. It indicates that the moisture inside the specimen is different from that of at the concrete surface in the cases of the specimens stored in outdoors. In this study, the moisture inside the specimens also affects the air permeability test in the case of the specimens stored in outdoors.

Based on this study, a combination of the air permeability test and electric resistivity test is a useful technique to evaluate the quality of the con-

crete cover in the structures. However, the scattering results are observed in the plain concrete specimens. Among all specimens with 0.60 of water-to-cement ratio, there is one specimen that shows very bad quality of concrete although they were produced under the same conditions. Because the scattering might also occur in the real structure, it is recommended to collect more number of data in the future.

6. Conclusions

To investigate the quality of insufficient concrete cover, MIP test was conducted. In addition, the air permeability test was carried out to verify the applicability of this test method to investigate the existence of the insufficient concrete cover. The conclusions obtained from this research are as follows.

- (1) Based on the MIP test, it is confirmed that in the case of insufficient concrete cover, the concrete properties in the concrete cover is different from that in center portion of the specimen in which the pore structure in this layer is coarser than in the center portion of the speci-

men. With thinner concrete cover, the pore structure becomes coarser. As the water-to-cement ratio decreases from 0.60 to 0.45, the pore structure becomes finer, and the difference in the pore structure between the concrete cover and the center portion becomes smaller. However, the pore structure in the concrete over the reinforcing bar is still coarser than that in the concrete at the center portion. The dominant pore size for the concrete at the center portion is smaller than that for the concrete cover indicating finer pore structure. It is concluded that when the concrete cover is insufficient, not only the distance needed for the substances to reach the steel bar becomes shorter, but also the pore structure becomes coarser. In this study, for example, the properties of the concrete cover in the case of 0.45 of water-to-cement ratio should be considered as the concrete properties with water-to-cement ratio which is higher than 0.60.

- (2) Although the changes in pore structure over time vary depending on the exposure conditions, the cumulative pore-size distributions and the derivatives of the curves for the specimens stored in outdoors are almost the same as those of the specimens stored in indoors at 91 days. It is confirmed that as the concrete cover is thinner, the change in pore structure in this thin layer is affected directly by the environmental condition. In the cases of the specimens stored in indoors, the main capillary pore in the thin layer is shifted to the bigger size which might be attributed to the drying condition, while the main capillary pore in the concrete over the reinforcing bar at cover depth of 30 mm and at center portion is shifted to the smaller size. In the cases of the specimens stored in outdoors, the main pore peak in the thin layer is shifted to the bigger size and large pores appear which might be caused by the relatively high temperature in summer from 7 days to 14 days. The large pores in the concrete over the reinforcing bar at cover depth of 30 mm and at the center portion do not occur as much as those in the thin layer. After 14 days, the volume of main pores decreases and the dominant pore size becomes smaller indicating hydration proceeds.
- (3) The air permeability test roughly pointed out the existence of the poor quality of the concrete cover in the cases of the insufficient concrete cover. The air permeability coefficients in the cases of 5 mm and 15 mm of concrete

cover are higher than those in the cases of thicker concrete cover. Thus, a combination of the air permeability test and electric resistivity test is a useful technique to evaluate the quality of the concrete cover.

- (4) The MIP test and non-destructive tests show the same tendency that poor quality of concrete is observed when the concrete cover is insufficient. Based on the MIP test, with deeper zone, the porosity becomes finer. The non-destructive tests measure the concrete cover quality as the average over a certain depth of the measurement.

Acknowledgement

This work was supported by Council for Science, Technology and Innovation (CSTI), Cross-ministerial Strategic Innovation Promotion Program (SIP), "Infrastructure Maintenance, Renewal, and Management Technology" (Funding agency: JST)

References

1. Polder, R.B.; and De Rooij, M.R. (2005) "Durability of marine concrete structures: field investigations and modeling," *Heron*, 50(3), pp. 133-152.
2. Moradi-Marani, F.; Shekarchi, M.; Dousti, A.; and Mohasher, B. (2009) "Investigation of corrosion damage and repair system in a concrete jetty structure," *Journal of Performance of Constructed Facilities*, 24(4), pp. 294-301.
3. DeSouza, S.J.; Hooton, R.D.; and Bickley, J.A. (1998) "A field test for evaluating high performance concrete covercrete quality," *Canadian Journal of Civil Engineering*, 25(3), pp. 551-556.
4. Basheer, L.; Kropp, J.; and Cleland, D.J. (2001) "Assessment of the durability of concrete from its permeation: a review," *Construction and Building Materials*, 15(2-3), pp. 93-103.
5. Akmal, U.; Hosoda, A.; Hayashi, K.; and Suhara, K. (2012) "A new surface water absorption test and its application," *Proceedings of the 14th International Conference on Structural Faults and Repair*, Edinburg, UK.
6. Torrent, R.J. (1992) "A two-chamber vacuum cell for measuring the coefficient of permeability to air of the concrete cover on site," *Materials and Structures*, 25(6), pp. 358-365.
7. Torrent, R. (2012) "Non-destructive air-permeability measurement: from gas-flow modeling to improved testing," *Proceedings of the 2nd International Conference of Micro-*

- structural-related Durability of Cementitious Composites, Amsterdam, Netherlands.
8. Sengul, O.; and Gjorv, O.E. (2008) "Electrical resistivity measurements for quality control during concrete construction," *ACI Materials Journal*, 105(6), pp. 541-547.
 9. Polder, R.B. (2001) "Test methods for on site measurement of resistivity of concrete-a RILEM TC-154 technical recommendation," *Construction and building materials*, 15(2), pp. 125-131.
 10. Beglarigale, A.; Ghajeru, F.; Yigiter, H.; and Yazici, H. (2014) "Permeability characterization of concrete incorporating fly ash," *Proceedings of the 11th International Congress on Advances in Civil Engineering*, Istanbul, Turkey.
 11. Neves, R.; Sena da Fonseca, B.; Branco, F.; de Brito, J.; Castela, A.; and Montemor, M.F. (2015) "Assessing concrete carbonation resistance through air permeability measurements," *Construction and Building Materials*, 82, pp. 304-309.
 12. Andrade, C.; Gonzalez-Gasca, C.; and Torrent, R. (2000) "Suitability of torrent permeability tester to measure air-permeability of covercrete," *Special Publication, International Concrete Abstracts Portal*, 192, pp. 301-318.
 13. Gjorv, O.E.; Vennesland, O.; and El-Busaidy, A.H.S. (1977) "Electrical resistivity of concrete in the oceans," *Proceedings of the 9th Annual Offshore Technology Conference*, Houston.
 14. Tuutti, K. (1982) "Corrosion of steel in concrete," *CBI*, pp. 1-159.
 15. Glass, G.K.; Page, C.L.; and Short, N.R. (1991) "Factors affecting the corrosion rate of steel in carbonated mortars," *Corrosion Science*, 32(12), pp. 1283-1294.
 16. Halamickova, P.; and Detwiler, R. (1995) "Water permeability and chloride ion diffusion in portland cement mortars: Relationship to sand content and critical pore diameter," *Cement and Concrete Research*, 25(4), pp.790-802.
 17. Yang, C.C. (2006) "On the relationship between pore structure and chloride diffusivity from accelerated chloride migration test in cement-based materials," *Cement and Concrete Research*, 36(7), pp. 1304-1311.
 18. Subcommittee on English Version of Standard Specifications for Concrete Structures (2007) "Standard specifications for concrete structures -2007 "Materials and Construction"," *Japan Society of Civil Engineers (JSCE)*, Tokyo, Japan.
 19. Torrent, R.; and Frenzer, G. (1995) "A method for the rapid determination of the coefficient of permeability of the "covercrete"," *Proceedings of the International Symposium Non-Destructive Testing in Civil Engineering (NDT-CE)*, Berlin, Germany.
 20. Kurashige, I.; Yamada, K.; and Ogawa, S. (2016) "Feasibility study on quality verification of casted concrete using nondestructive air permeability test and electric resistivity measurement toward radioactively contaminated waste disposal," *Cement Science and Concrete Technology*, 69(1), pp. 287-294.
 21. Hilsdorf, H.; and Kroop, J. (1995) "Performance criteria for concrete durability," *Chapman & Hall*, pp. 336.